ELSEVIER

Chemical Engineering and Processing 41 (2002) 99–106

Chemical Engineering and Processing

www.elsevier.com/locate/cep

Hydrodynamics of a swirling fluidised bed

Binod Sreenivasan [a,*], Vijay R. Raghavan [b]

[a] *Department of Engineering, University of Cambridge, Trumpington Street, Cambridge CB2 1PZ, UK*
[b] *Department of Mechanical Engineering, Indian Institute of Technology, Madras 600036, India*

Received 12 July 2000; received in revised form 23 November 2000; accepted 23 November 2000

Abstract

A novel variant of the fluidised bed, the swirling fluidised bed, featuring an annular bed and inclined injection of gas through the distributor blades, is studied in the present work. The hydrodynamic characteristics in the swirling regime of operation are studied in detail, experimentally as well as by an analytical model. Unlike a conventional bed, the swirling bed presents three, or sometimes four regimes of operation depending on the bed weight. Bed pressure drop studies have been carried out in a swirling bed for two different sizes of spherical PVC particles. A striking feature that distinguishes the swirling bed from a conventional fluidised bed is that, the bed pressure drop in the swirling mode, $(\Delta p)_{b,s}$ increases with air velocity. A physically plausible explanation for this behaviour is that, $(\Delta p)_{b,s}$ is proportional to the centrifugal weight of the bed. This idea leads to the development of an approximate model that predicts the mean angular velocity of the bed, and hence, $(\Delta p)_{b,s}$, at a given air flow rate. The good agreement between the theoretical and experimentally obtained $(\Delta p)_{b,s}$ values at moderate air flow rates, and the results of an uncertainty analysis performed on the model indicate that the present model describes the fluidised regime of a swirling bed satisfactorily.

Keywords: Fluidised bed; Swirling regime; Pressure drop

1. Introduction

The problem of inadequate lateral mixing of solids and gas–solids contacting in shallow fluidised beds can be overcome in many ways. Merry [1] studied the horizontal injection of a gas jet into a conventional fluidised bed, with the effect of generating a swirl motion of the particles entrained in the path of the jet. Researchers in the past [2–4] have been experimenting with centrifugal fluidised beds, wherein the centrifugal weight of the particles is balanced by the pressure drop of gas flowing radially inward into the bed. Equipment using the swirling bed principle appears to be commercially available for operations such as drying, granulation and exfoliation, but published information on the behaviour of such beds is scanty. Inclined injection of gas has been employed in the 'Conidur' plate distributors. Two semi-circular plates are welded along the diameter. In each half, gas enters through conical slits at an angle close to the horizontal, but in opposite directions in order to create large scale mixing, which is very useful in fluid bed equipment for drying, cooling or ventilation of powder or granulated products. An early work on inclined injection of gas into a fluidised bed of particles, using a plate with punched slits, so as to produce a tangential motion, was carried out at Aston University in Birmingham [5]. As in the case of the spiral distributor developed by Ouyang and Levenspiel [6], the work was performed on a full diameter distributor. The results were perhaps not spectacular to merit further research interest. The change from a full width column to an annular column however renders a remarkable change in bed behaviour. Though no research papers have appeared, this concept has already found use in industrial equipment. The 'Torbed' reactor technology, which originated in the UK, features a ring of fixed, angled blades located at the bottom of the reactor, through which the process gas is circulated. The toroidal mixing motion of the particles ensures high heat and mass transfer rates. The first application of this technology was in vermiculite mineral exfolia-

* Corresponding author. Tel.: +44-1223-766289.
E-mail address: bs229@eng.cam.ac.uk (B. Sreenivasan).

0255-2701/02/$ - see front matter
PII: S0255-2701(00)00155-0

tion to produce insulating and fire-retardant board. Now, this reactor is a popular choice for processes that require precise gas–solids contact such as roasting, calcination, desorption, dissociation etc.

The swirling fluidised bed studied in the present work is similar to the Torbed reactor, in that, it features an annular bed and inclined injection of gas through the distributor blades, resulting in a swirling motion of solid particles in a confined circular path. When a jet of gas enters the bed at an angle θ to the horizontal, the vertical component of the velocity, $v \sin \theta$, causes fluidisation, and the tangential component, $v \cos \theta$, is responsible for the swirl motion of the bed material. As the gas penetrates deeper into the bed, its horizontal momentum is attenuated, and it finally dies out at a certain height above the distributor, if the bed is sufficiently deep. If the bed is shallow enough, the velocity of the gas leaving the bed will still have two components. In this case, the bed will be a single swirling mass. Use of a lower angle of injection ensures vigorous mixing of solids and hence, high transport coefficients. The gas velocity can be increased to high values with little carry-over of particles because the vertical component of the velocity is only a fraction of the jet velocity.

The swirling bed apparatus studied in the present work holds promise for industrial application for kinetics controlled processes, drying of foundry sand being one example. It also has potential for treating of temperature sensitive materials. Drying of black pepper is such an example where the high porosity of pepper and the high transport coefficients between gas and particles make rapid drying possible without degradation.

In Section 2, we present the salient features of the swirling fluidised bed in the various regimes of operation. The experimental investigations on the bed pressure drop in the swirling mode reveal the interesting trend of the pressure drop increasing with air velocity. In Section 3, an analytical model that predicts the bed pressure drop in the swirling regime of the bed is developed. The model rests on two principal assumptions: (a) the bed is a single swirling mass and (b) there is no slip between the gas and the particles at the free surface of the bed. If the net torque imparted to the particles by the fluidising gas is sufficient to overcome the rates of change of angular momentum due to friction at the wall and the distributor, a bed of given mass is subject to swirl motion. From the above reasoning, the angular velocity of the bed, ω, and hence, the pressure drop are predicted. The model is strengthened further by an uncertainty analysis, wherein the observed error in the estimation of the pressure drop can be used to determine the error in the estimation of ω. In the concluding section, we comment on the agreement of our theoretical estimates with the experimental data in the fluidised regime, and discuss the scope for future work.

2. Experimental study

2.1. Experimental set-up and procedure

The schematic diagram of our test rig is given in Fig. 1. The unit consists of a Plexiglas column enclosing a Plexiglas cylinder that forms the bed wall. The column and the bed are mounted on the distributor. The *annular spiral distributor* used in this bed is a variant of the spiral distributor developed by Ouyang and Levenspiel [6]. But, unlike the spiral distributor, wherein overlapping blades shaped as full sectors of a circle are welded together at the centre of the bed, the annular distributor is made of a number of blades that are truncated sectors of a circle, as shown in Fig. 2. Sixty such blades are arranged at an angle of 12° to the horizontal with the help of two Plexiglas outer and inner holders, by cutting a slot in each holder. The inner holders are arranged around a Bakelite disk of diameter 200 mm at the centre. The overlapping length between the blades directs the air at the designed angle. The gap between two blades is not uniform, but varies in proportion to the radius, thereby creating a trapezoidal opening for air flow. The air gap for the present configuration is 1.18 mm at the inner radius and 2.27 mm at the outer radius.

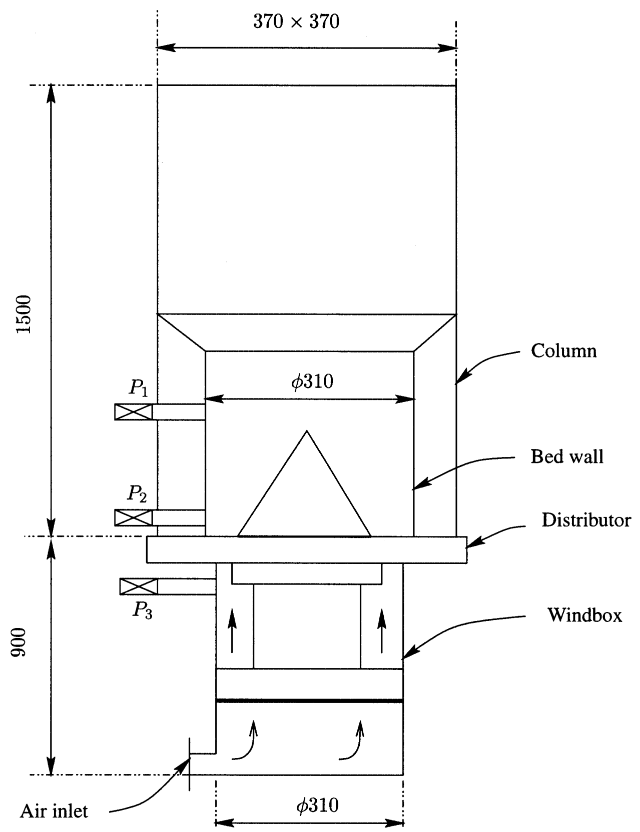

Fig. 1. Schematic of the experimental set-up.

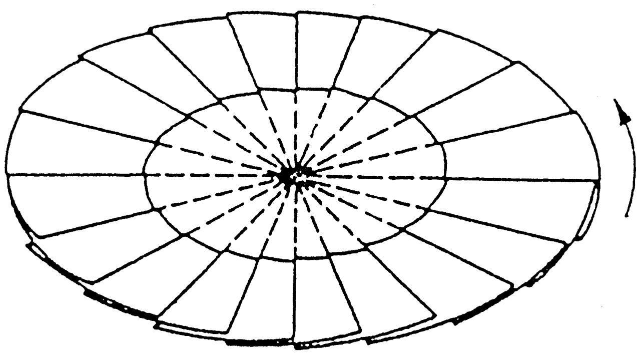

Fig. 2. The annular spiral distributor. The air flow is in the counter-clockwise direction.

A hollow metal cone is centrally located at the base of the bed. In the presence of a cone at the bed centre, the superficial velocity of the gas decreases continuously from the distributor to the free surface of the bed, owing to the increasing cross-section available for air flow. Hence, one could operate relatively deeper beds at high velocities without the problem of particle elutriation. The cone also eliminates the possible creation of a 'dead zone' at the centre of the bed.

The air flow rate through the bed is obtained by measuring the pressure drop across a venturi flowmeter. Three pressure tappings, P_1, P_2 and P_3 are provided on the set-up, two on the bed wall and one on the windbox below the distributor plane. The distributor pressure drop, P_2-P_3 is measured at different air flow rates, in an empty bed. The bed pressure drop is then obtained by subtracting the distributor drop from the total pressure drop, P_1-P_3. All pressure drops were measured in mm of water using digital as well as water manometers.

After loading the bed with a known weight of particles, the air flow was increased progressively and the venturi and total pressure drops were noted at each step. Experiments were performed with spherical PVC particles of two sizes, 3.5 and 2.5 mm. The various regimes observed are given briefly in the next section.

2.2. Bed behaviour

A detailed qualitative description of the bed behaviour can be found in [7]. As the flow rate is increased, we come across the following regimes:

1. Bubbling
2. Wave motion with dune formation: A localised swirl motion is initiated at any random location in the bed. Swirling extends over a certain arc of the bed, while the remaining arc is static. The swirling zone carries the particles with it and deposits them at the boundary of the static zone. At the other boundary of the static zone, material gets depleted due to the same swirling zone, thereby reducing the bed height at the boundary and triggering a second swirl motion. Thus, at one end of the swirling arc, the static region grows, and at the other end, it decays.
3. Two-layer fluidisation: This is observed only in deep beds. We have observed this regime only when the static bed height was greater than 45 mm. When the *minimum two-layer velocity* is reached, a thin continuously swirling lower layer and a vigorously bubbling top layer is visible. It is clear that the azimuthal component of the velocity vanishes at the interface between the two layers.
4. Stable swirling: On further increasing the air velocity, one can observe that the dune formation is attenuated, the swirling region gets wider, and finally, the dune disappears to present a fully swirling bed. In this phase, the bed can be considered fluidised because a heavier object sinks in the bed, and particles smoothly flow out when a weir built on the bed wall is opened. In the swirling mode, the free surface of the bed resembles somewhat that of a rotating fluid, with a higher bed height at the wall than in the centre of the bed. The analogy to a rotating fluid is however not rigid. In a fluid rotating due to a rotation of the containing vessel, the entire mass of fluid will be forced to rotate with the same angular velocity and the inner to outer height may vary less or more, depending on the ratio of inner to outer diameter and the speed of rotation. On the other hand, in the swirling bed where the swirling is generated by the gas flow, the angular velocity decays upwards and does not give rise to as drastic changes in the level of the bed as would be expected with a liquid. Further, the ratio of the annulus width to outer diameter is only about 1/6. This does not give rise to any serious disparity in centrifugal forces at the inner and outer periphery. For the range of operating velocities considered in the present work, a smoothly swirling bed with a turbulence-free top surface has been observed. At higher velocities, the swirling particles are displaced to the wall region due to the strong outward centrifugal force developed. The annular distributor serves to reduce the radial variation in the centrifugal force, as compared to a full circular distributor. In this operating mode, we have found that one layer of particles adheres to the column wall due to the electrostatic charge developed between PVC and Plexiglas. Though this may be a special feature found only in the set-up used for the present study, we consider it necessary to account for the fraction of the mass of particles adhering to the bed wall, in the model presented in Section 3. This fraction does not have to be supported by the fluidising gas, and does not contribute to the friction losses at the distributor.

Table 1 summarises the behaviour of a 0.5-, 1.0- and 1.5-kg bed of 3.5-mm particles. The *superficial velocities* in m s^{-1} are obtained by dividing the measured air flow rate by the distributor ring area. Interestingly, the minimum bubbling velocity values compare well with the calculated *minimum fluidisation velocity* of 1.09 m s^{-1} obtained from a correlation recommended by Chitester et al. [8] for coarse particles, in a conventional bed:

$$\mathrm{Re}_{\mathrm{p,\,mf}} = [(28.7)^2 + 0.0494\ \mathrm{Ar}]^{0.5} - 28.7, \tag{1}$$

where Ar is given by

$$\mathrm{Ar} = \frac{d_\mathrm{p}^3 \rho_g (\rho_\mathrm{p} - \rho_g) g}{\mu_g^2}. \tag{2}$$

The density of the particle used is 1100 kg m^{-3}.

Though air enters the bed at an angle, the behaviour of the bed in the packed regime is similar to that of a conventional bed, since the kinetic energy of air flow is not sufficient to unlock the particles and create swirl. The jet of air dissipates the same way as it does at the distributor in a packed bed and percolates through the interstices. This situation continues only up to the appearance of bubbles in the bed, which occurs practically at the minimum fluidisation velocity of a conventional bed. We also notice that, the larger the bed weight, higher the minimum swirl velocity. As the bed weight increases, the air has to impart a greater momentum to overcome the wall and distributor friction, both of which, as we shall see in Section 3, are functions of the bed weight.

2.3. Bed pressure drop

Fig. 3 presents the measured bed pressure drop, $(\Delta p)_\mathrm{b}$, for two different sizes of spherical PVC particles, in mm of water. The Ergun equation [9], generally used for packed beds, predicts the pressure drop in the packed regime of our bed to within 20% of the experimental values. For a smaller particle size, both the viscous and kinetic energy losses are greater; and hence, $(\Delta p)_\mathrm{b}$ in the packed regime is higher. In the regime of wave motion, the pressure drop does not remain stable because the bed height at any location fluctuates continuously between a maximum and minimum. This unstable zone of operation, between bubbling and stable swirling, does not lend itself to simple physical modelling. The fully swirling regime, which is of primary interest to us in this work, presents a picture quite different from what is seen in a conventional fluidised bed in the fluidised regime. The bed pressure drop increases with air flow rate. This means that, in addition to the weight of the bed, there must be a downward-acting force, the magnitude of which increases with velocity. Here, we propose that this extra force be due to wall friction, contributed by the centrifugal weight of the bed acting normal to the wall. This force increases with velocity, and opposes the upward motion of particles during bed expansion. Based on the above reasoning, we model the pressure drop, $(\Delta p)_{\mathrm{b,s}}$, in the swirling regime of operation.

Table 1
Features of the bed in the various regimes of operation

	Bed weight (kg)		
	0.5	1.0	1.5
Static bed height (mm)	22	42	59
Minimum bubbling velocity (m s^{-1})	1.07	1.19	1.23
Minimum velocity for wave motion (m s^{-1})	1.34	1.55	1.71
Minimum two-layer velocity (m s^{-1})	–	–	2.22
Minimum swirl velocity, U_ms, (m s^{-1})	2.13	2.54	3.03
Expanded bed height at U_ms, mm	33	72	110

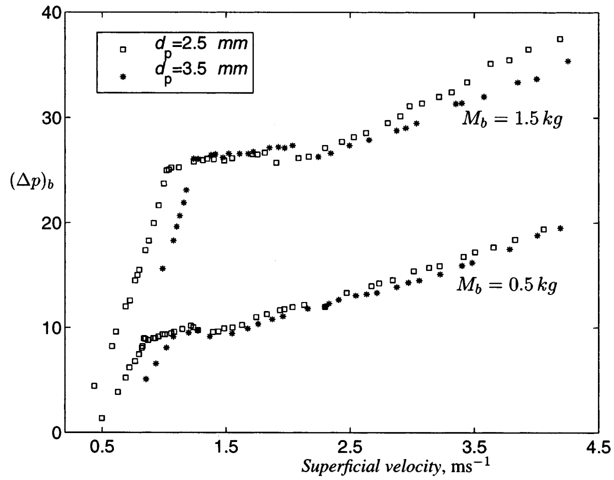

Fig. 3. Experimentally obtained bed pressure drop, in mm of water.

3. Prediction of bed pressure drop in the swirling regime

In this section, we develop a simple analytical model that predicts $(\Delta p)_{\mathrm{b,s}}$. According to the reasoning in Section 2.3, the magnitude of the centrifugal weight of the bed must be known in order to obtain the pressure drop at any flow rate. Therefore, we first need to derive the angular velocity of the bed at a given aeration rate. The principal assumptions that we use in the formulation are, (a) the bed is a single swirling mass of uniform angular velocity, and (b) the angular velocity of gas at the free surface of the bed is approximately equal to the mean angular velocity of the bed, ω. In other words, a no-slip condition is assumed to exist at the free surface of the bed. In addition, since the spacing between two blades is of trapezoidal cross-section, the mass flow rate of gas between them, $\dot{m}$, can be assumed to vary linearly with the radial position along the blade, so that,

$$d\dot{m} = c_1 dr. \tag{3}$$

Likewise, the total mass flow rate at any section of the bed, M, can be assumed to vary linearly as the flow area:

$$d\dot{M} = c_2 dA = 2\pi c_2 r dr. \tag{4}$$

We invoke the principle of conservation of angular momentum to state the following semantic equation: Net rate of change of angular momentum of gas between inlet and free surface

= Moment due to wall friction +
Moment due to distributor friction. (5)

3.1. Rate of change of angular momentum of gas

The net rate of change of angular momentum experienced by the fluidising gas as it passes through the bed is given by

$$\dot{H} = n_b \int_{r=r_i}^{r_o} d\dot{m} v_{\theta,\mathrm{i}}\, r - \int_{r=r_i'}^{r_o} d\dot{M} v_{\theta,\mathrm{e}}\, r \tag{6}$$

where n_b is the number of blades, $v_{\theta,\mathrm{i}}$ is the tangential velocity of gas at the inlet (given by $v \cos\theta$), $v_{\theta,\mathrm{e}}$ is the tangential velocity at the free surface of the bed, and r_i, r_i' and r_o are the radii shown in Fig. 4. Using our principal assumptions, Eq. (6) can be simplified as follows:

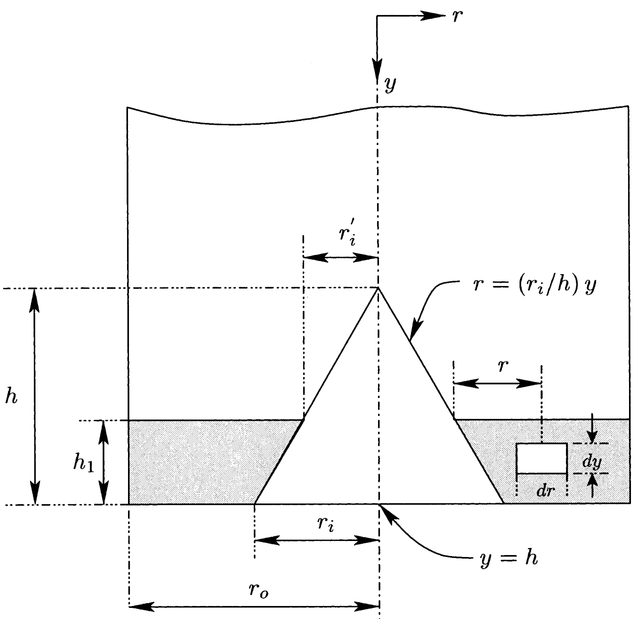

Fig. 4. Bed geometry in the swirling mode of operation.

$$\dot{H} = \dot{M} v_{\theta,\mathrm{i}} (r_i + r_o)/2 - \dot{M}(r_o^2 + r_o'^2)\omega/2. \tag{7}$$

3.2. Moment due to wall friction

The centrifugal weight, W_c, of the bed with a cone at the centre is given by (see Fig. 4)

$$W_c = \int_{y=h-h_1}^{h} \int_{r=(r_i/h)y}^{r_o} 2\pi\omega^2 \rho_b r^2 \,dr\, dy, \tag{8}$$

which simplifies to

$$W_c = \frac{2}{3}\pi\omega^2\rho_b \left\{ r_o^3 h_1 - \frac{r_o^3}{4} h\left[1 - \left(\frac{h_1}{h}\right)^4\right]\right\}, \tag{9}$$

where ρ_b is the bulk density of the swirling bed, evaluated from the bulk volume of the bed in the expanded state. The wall friction moment is then given by

$$\mathscr{M}_w = W_c \mu_w r_o. \tag{10}$$

3.3. Moment due to distributor friction

The distributor friction depends on the actual weight of the bed acting on the distributor. As mentioned earlier in Section 2.2, one layer of particles adheres to the Plexiglas wall during stable swirling. The effective weight of particles supported by the distributor can be estimated approximately as follows: If n is the number of particles per unit length, then $n = 1/d_p$. Assuming uniform packing, the number of particles per unit volume is n^3. Let n'^3 be the number of particles in the expanded state of the bed. Then,

$$n' \approx n(v_e/v_p)^{-1/3}, \tag{11}$$

where v_p and v_e are the volumes of the bed in the packed and expanded states. Now, the total number of particles wetting the wall surface in the swirling regime, n_{pw} is $2\pi r_o h_1 n'^2$. If n_p is the total number of particles in the bed (estimated from the mass of the bed and the mass of one particle), then the fraction of the bed weight, k, actually supported by the fluidising gas is given by

$$k = 1 - \frac{n_{pw}}{n_p}. \tag{12}$$

For a particle diameter of 3.5 mm, this factor is 0.9, with slight variations with bed weight. The moment due to distributor friction, $\mathscr{M}_d$, is estimated as

$$\mathscr{M}_d = \int_{r=r_i}^{r_o} k M_b g \mu_d r (\mathrm{d}A/A) \tag{13}$$

which simplifies to

$$\mathscr{M}_d = \frac{2}{3} k M_b g \mu_d \left(\frac{r_o^3 - r_i^3}{r_o^2 - r_i^2}\right). \tag{14}$$

Substituting the values of the expressions in Eqs. (7), (10) and (14) in Eq. (5), a quadratic equation in ω is obtained, which on solving, yields the angular velocity of the bed. The input parameters for this model, such as the bed weight, height and the jet velocity through a pair of blades are obtained experimentally [7]. The dynamic friction coefficients, μ_w and μ_d, when assigned values of 0.25 and 0.15 respectively, gave an excellent match between the theoretical and experimental pressure drop values. These values are acceptable for friction between the PVC particles and the Plexiglas wall and the metallic distributor plate.

For a 0.5-kg bed, our model for ω predicts an *average* angular velocity of 1 revolution per second (or 2π rad s^{-1}) at an air superficial velocity of 2.1 m s^{-1}. For a 1-kg bed, the same rotational speed is attained at $u = 2.8$ m s^{-1}, and for a 1.5-kg bed, this speed is attained only at $u = 3.4$ m s^{-1}. The ω values obtained are directly used in the estimation of bed pressure drop in the swirling regime.

3.4. Estimation of $(\Delta p)_{b,s}$

The mean area available for air flow through the bed, a_m, can be obtained as an average of the ring areas of the distributor and the free surface of the bed. The theoretical pressure drop at fluidisation may be expressed as

$$(\Delta p)_{fl} = kM_b/a_m. \tag{15}$$

The factor k has been defined in Eq. (12). The pressure drop in the swirling regime can be written in the following form:

$$(\Delta p)_{b,s} = (\Delta p)_{fl} + \psi\omega^2, \tag{16}$$

where ψ is a constant obtained from Eq. (9). The first term on the right hand side of Eq. (16) represents the actual weight supported, and the second term, the contribution of the centrifugal force towards increment in pressure drop.

Fig. 5 gives the comparison between the predicted and experimental pressure drop values in the swirling regime in a bed of 3.5 mm particles, with cone as the centre-body. A maximum deviation of 5% is observed for the case of a 1.5-kg bed. The dotted lines correspond to the calculated pressure drop at minimum fluidisation, given by Eq. (15).

3.5. Uncertainty analysis

If $(\Delta p)_{b,s}$ is denoted by X for convenience, Eq. (16) can be re-written as

$$X = kM_b/a_m + \psi_1(\mu_w/a_m)\omega^2 \tag{17}$$

where ψ_1 is another constant. Hence,

$$\omega = [(Xa_m - kM_b)/\mu_w\psi_1]^{1/2}. \tag{18}$$

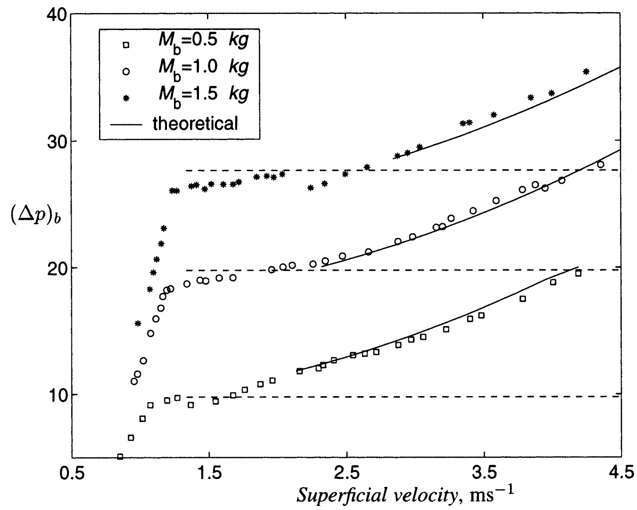

Fig. 5. Comparison of theoretical and experimentally obtained bed pressure drop values in the swirling regime. The values are given in mm of water. The dashed lines correspond to the $(\Delta p)_{fl}$ values.

The uncertainty in the predicted value of ω that would ultimately result in an error of σ_x observed in the bed pressure drop can be derived from Eq. (18) as follows:

$$\sigma_\omega^2 = \left(\frac{\partial\omega}{\partial X}\right)^2\sigma_X^2 + \left(\frac{\partial\omega}{\partial a_m}\right)^2\sigma_{a_m}^2 + \left(\frac{\partial\omega}{\partial\mu_w}\right)^2\sigma_{\mu_w}^2 + \left(\frac{\partial\omega}{\partial k}\right)^2\sigma_k^2 \tag{19}$$

where σ is the absolute error in the respective quantity. Here, we assume that a_m, μ_w and k are prone to uncertainties. The above equation can be re-written by substituting the values of the partial derivatives and working with relative errors. The algebra is straightforward and is not reproduced here. In order to ascertain the influence of the second, third and fourth terms on the right hand side of Eq. (19) on the uncertainty in ω, two of them may be kept equal to zero and the third may be varied. It is seen that a variation in σ_{a_m}/a_m does not have any appreciable influence on σ_ω/ω, and for a given value of $\sigma_{\mu_\omega}/\mu_\omega$, σ_ω/ω has a constant value over the entire velocity range in the swirling regime. The effect of σ_k/k on σ_ω/ω is interesting, in that, for any given value of σ_k/k, σ_ω/ω has unrealistically high values at low velocities, drops to a low value within a narrow range, and thereafter decreases only gradually. Fig. 6 shows the trend for two different bed weights, when $\sigma_k/k = 2\%$. The x-axis is normalised with respect to the minimum swirl velocity (U_{ms}) values obtained experimentally. The swirling regime commences only at these velocities, so the k factor, and σ_k have physical significance only at higher velocities. We can thus approximately identify the swirling mode of operation as that region for which the variation of σ_ω/ω is small. The present model can be considered valid only in this regime.

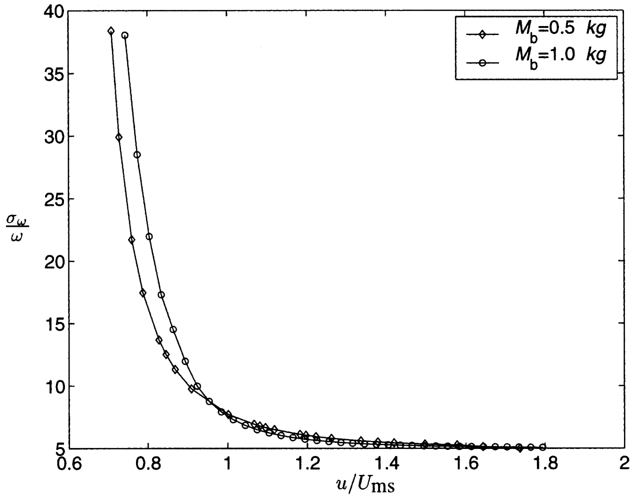

Fig. 6. Expected error (%) in the estimation of ω as a function of superficial velocity.

4. Discussion

In the present work, the hydrodynamic characteristics of a swirling fluidised bed have been studied experimentally, as well as by a simple analytical model. Unlike in a conventional bed, which has only two regimes of operation, one can demarcate three, sometimes even four regimes of operation in a swirling fluidised bed. For deep beds, a two-layer fluidisation regime, with a lower swirling layer and a top bubbling layer precedes the fully swirling regime. The existence of the two-layer bed shows that the tangential component of the velocity decays and drops to zero at a certain height. However, in order to derive maximum advantage of the swirl motion of particles, the bed appears more suited for operation in the shallow mode.

It has been found experimentally that the pressure drop in the swirling regime is not constant, but increases with gas flow rate. It is proposed that the pressure drop increases with centrifugal weight of the bed, or in simple terms, the angular velocity of particles. We have developed an analytical model to predict the angular velocity of the bed. The model assumes that the bed is a single swirling mass with zero slip between gas and particles at the free surface. These assumptions appear well-founded from the good agreement obtained between the predicted and experimental values of the bed pressure drop in the swirling regime, as seen in Fig. 5. It would be, however, erroneous to apply the model to relatively deep beds, which are turbulent swirling beds without a well-defined free surface, because the assumption of no-slip at the top surface becomes questionable. A major advantage of this global model is that the momentum loss due to inter-particle collision need not be accounted for. As one particle loses momentum due to a collision, another particle will gain the same momentum, assuming elastic impact.

When attributing the increase of the bed pressure drop to the increasing angular velocity of the bed material, it is also necessary to preclude other possible explanations for this interesting behaviour. For instance, it may be argued that the distributor plate may rearrange the flow in the swirling regime of operation, causing a variation in pressure drop. It may be recalled that the pressure drop has been measured for the empty column and the bed at the *same* superficial velocity, before the bed pressure drop is arrived at by subtraction. The possibility of occurrence of a radially distributed velocity is remote for the annular distributor, for reasons mentioned in Section 2.2. If a skewed velocity distribution did exist, there would be less flow along the wall and more along the inner periphery. The pressure drop readings taken at the wall would then be lower, and not higher as observed. Moreover, if the flow was redistributed, then the outer layers receiving less flow should de-fluidise; in other words these layers should de-swirl. This is certainly contrary to our observation.

In the uncertainty analysis given in Section 3.5, we use the *known* values of the error in $(\Delta p)_{b,s}$ to calculate the error in the estimation of ω as a function of gas flow rate. The values of the error obtained when the velocity is less than the minimum swirl velocity are not realistic. When $u > U_{ms}$, the error in ω is acceptable. The error analysis, in conjunction with experimental data, thus specifies the region of validity of the present model.

Fig. 5 tells us that the pressure drop in the swirling regime is always greater than the calculated pressure drop due to bed weight per unit area, given by Eq. (15). We infer that the bed in the swirling mode is essentially fluidised. This fact has been confirmed by visual observation.

The swirling action of the bed overcomes certain particular shortcomings of the conventional shallow bed. In the swirling zone, no bubbles are seen and no gas bypassing occurs. Due to its helical path the gas has a slightly longer travel than the bed height. Particle circulation does not depend on the bubbles. The feed, at one point of the swirling bed, disperses quickly and thoroughly in the bed.

It is commonly seen in fluidised bed literature that the distributor pressure drop needs to be quite high for uniform fluidisation. This is another favourable aspect of swirling fluidisation that large open area fractions and low pressure drops at the distributor can be employed without ill-effects. Any gas jets formed at the distributor openings are quickly smothered by the cross flow of particles and no stable jet formation can be seen.

Against these advantages the question of scale-up must be set. The variation of centrifugal forces along the radius might seem to present an impediment to enlarging these beds. For a given superficial velocity of gas, the angular velocity is expected to be lower at larger radii. However, there is a toroidal particle motion superimposed on the circumferential path of the particles. The toroidal motion further mixes particles in the radial direction and tends to equalise the particle momentum. It would then be reasonable to expect that the usable bed height will not be a strong function of the diameter.

The physical size of the swirling bed does not limit the throughput on account of the great rapidity of material processing. One contra-indication for the use of these beds is of course in diffusion-controlled processes. The vigorous swirling action of the bed is ineffective in such applications.

There is enough scope for interesting theoretical and experimental studies on the hydrodynamics of swirling fluidised beds. For instance, the influence of angle of injection, θ, on the bed behaviour can be studied. As θ is increased, the advantage derived from the swirl motion of particles diminishes, but the pressure drop in the fluidised regime also decreases owing to the lower centrifugal weight of the particles. Further, the complex regime of *wave motion with dune formation* needs to be studied in detail. Only a qualitative assessment of the bed behaviour has been possible so far. Operation in this regime can conserve gas use. This region may be of interest for processes where the controlling resistance is on the solids side.

Appendix A. Nomenclature

a	area (m^2)
Ar	Archimedes number
d	diameter (m)
g	acceleration due to gravity (m s^{-2})
H	angular momentum (kg m^2 s^{-1})
k	fraction of the bed weight supported by fluidising gas
$\dot{m}$	mass flow rate between two blades (kg s^{-1})
$\dot{M}$	total mass flow rate (kg s^{-1})
M	mass (kg)
$\mathscr{M}$	moment (N m)
Re	Reynolds number
u, U	velocity (m s^{-1})
v	jet velocity between blades (m s^{-1})
(Δp)	pressure drop (mm of water)
Greek	
μ	friction coefficient, dynamic viscosity of gas (N s m^{-2})
ρ	density (kg m^{-3})
σ	absolute error
ω	angular velocity (rad s^{-1})
Subscripts	
b	bed
b,s	bed in the swirling regime
c	centrifugal
d	distributor
fl	fluidised
g	gas
m	mean
mf	minimum fluidisation
ms	minimum swirl
p	particle
p,mf	based on particle diameter, minimum fluidisation
w	wall
θ	tangential

References

[1] J.M.D. Merry, Penetration of a horizontal gas jet into a fluidised bed, Trans. Inst. Chem. Eng. 49 (1971) 189.
[2] T. Takahashi, Z. Tanaka, A. Itoshima, L.T. Fan, Performance of a rotating fluidised bed, J. Chem. Eng. Jpn. 17 (1984) 333.
[3] L.T. Fan, C.C. Chang, Y.S. Yu, Incipient fluidisation condition for a centrifugal fluidised bed, AIChE J. 31 (1985) 999.
[4] Y.M. Chen, Fundamentals of a centrifugal fluidised bed, AIChE J. 33 (1987) 722.
[5] J.R. Howard (formerly at Aston University, presently at MIT), personal communication.
[6] F. Ouyang, O. Levenspiel, Spiral distributor for fluidised beds, Ind. Eng. Chem. Process Des. Dev. 25 (1986) 504.
[7] S. Binod, Hydrodynamic and wall–bed heat transfer studies on a swirling fluidised bed, Masters Thesis, Department of Mechanical Engineering, IIT, Madras, 1995.
[8] D.C. Chitester, R.M. Kornosky, L.S. Fan, Characteristics of fluidisation at high pressure, Chem. Eng. Sci 39 (1984) 253.
[9] S. Ergun, Fluid flow through packed columns, Chem. Eng. Progress 48 (2) (1952) 504.